A Letter-Of-Intent to Jefferson Lab PAC32

A Detailed Study of Semi-Inclusive Deep-Inelastic Pion Productions on Unpolarized Proton and Deuteron Targets with the CLAS12 Detector

R. Gilman, C. Glashausser, X. Jiang (Spokesperson)[a], G. Kumbartzki, R. Ransome.
Rutgers University, Piscataway, New Jersey.

Y. Jiang, H. Lu (Co-spokesperson), Y. Ye
University of Science and Technology of China, Hefei, P.R.China.

H. Avakian
Jefferson Lab, Newport News, Virginia.

Abstract: We propose a detailed study of event-multiplicity, azimuthal angle and transverse-momentum dependence of semi-inclusive deep-inelastic pion production with 11 GeV (and 8.8, 6.6 GeV) electron beam scattering off unpolarized proton and deuteron targets using the large acceptance CLAS12 detector. The goal of this experiment is to firmly establish the kinematic region over which SIDIS pion productions can be reliably interpreted to the Next-to-Leading-Order QCD in terms of parton distributions and parton fragmentation functions. The high precision data from this experiment, spanning over a dense 3D-grid of (x, Q^2, z) and a large enough P_t range, will be used as inputs to the next generation NLO global analysis, which includes world's data of unpolarized and polaried SIDIS as well as e^+e^- and pp reactions, to strongly constrain parton fragmentation functions, parton density and helicity distributions. This experiment will lay the groundwork of interpretations for the ambitious JLab 12 GeV SIDIS physics program, which include quark spin-flavor decomposition, polarized and Unpolarized sea asymmetry, transversity and Sivers function measurements and other transverse-momentum dependent parton distributions (TMDs) such as the Boer-Mulders function. This experiment can be staged as the CLAS12 commisioning experiment.

[a]Contact person, email: jiang@jlab.org

Contents

1 Introduction **4**
- 1.1 Semi-inclusive deep inelastic scattering . . . 4
- 1.2 Opportunities of SIDIS experiments at JLab 12 GeV . . . 5
- 1.3 Interpretations of SIDIS data . . . 5
- 1.4 The goal of this experiment . . . 6

2 Physics motivations **7**
- 2.1 Spin-independent semi-inclusive DIS cross sections at NLO . . . 7
- 2.2 NLO global fit of fragmentation functions. . . . 8
- 2.3 Experimental observables of this experiment . . . 10
  - Pion multiplicities . . . 10
  - Ratios of charged pion multiplicities . . . 10
  - Combined charged pion multiplicities . . . 10
  - Ratios of proton over deuteron combined charged pion multiplicities 10
  - SIDIS cross sections . . . 11

3 This Experiment **11**
- 3.1 The CLAS12 detector . . . 11
- 3.2 Electron detection . . . 11
- 3.3 Hadron detection . . . 11
- 3.4 Hadron phase space differences . . . 11
- 3.5 Vertex reconstruction . . . 11
- 3.6 Targets density and luminosity corrections . . . 11
- 3.7 Trigger and background . . . 11
- 3.8 Kinematic coverage of SIDIS reaction with the CLAS12 detector . . . 11

4 Event Rate Estimate and Projected Uncertainties **16**
- 4.1 Cross section and rate estimate . . . 16
- 4.2 Statistics compared with HERMES data . . . 16
- 4.3 Systematic uncertainties . . . 16
  - Relative systematic uncertainties . . . 16

5 Luminosity and beam time assumptions **16**

6 Expected Results **17**
- 6.1 SIDIS pion multiplicities, z-dependence . . . 17
- 6.2 Q^2 dependence of pion multiplicities . . . 17
- 6.3 Ratios of combined charged-pion multiplicities . . . 17
- 6.4 $P_\perp$ dependence of pion production . . . 17
  - $P_\perp$ dependence of the fragmentation functions . . . 17
- 6.5 Singlet and non-singlet fragmentation functions . . . 17
- 6.6 Valence quark distribution ratio d_v/u_v . . . 17

7 By-products **17**
7.1 SIDIS charged kaon multiplicities, z-dependence 17
7.2 $\cos\phi$ and $\cos 2\phi$ moments 17
7.3 Multiplicities of ρ, K_s^0 and ϕ mesons 17
7.4 Multiplicities of p, $\bar{p}$, Λ and other hyprons 17
7.5 Beam single-spin asymmetry A_{LU} 17
7.6 Absolute cross sections 17

8 Relation with other experiments **17**

9 Summary **23**

10 Acknowledgment **23**

A Details of Monte Carlo simulations **24**

1 Introduction

1.1 Semi-inclusive deep inelastic scattering

The last four decades has seen remarkable progress in our knowledge of the parton density $q_f(x)$ and polarization distributions ($\Delta q_f(x)$). The most precise and clearly interpreted data are from inclusive deep-inelastic lepton scattering (DIS) experiments at CERN, SLAC and DESY. However, the information available from inclusive DIS process has inherent limitations. As the cross sections are only sensitive to e_q^2, the quark charge square, an inclusive experiment probes quarks and anti-quarks on an equal footing, and it is only possible to determine combinations of $q_f(x) + \bar{q}_f(x)$, but never $q_f(x)$ and $\bar{q}_f(x)$ separately.

The sensitivity to each individual quark flavor is realized in semi-inclusive deep inelastic scattering (SIDIS) in which one of the leading hadrons is also detected. Since the leading hadrons from the current fragmentation are most likely to be correlated with the flavor of the struck quark, detection of the leading hadron effectively "tags" the struck quark. Therefore, SIDIS offers an unique opportunity for determining the spin, flavor, and sea structure of the nucleon [1], thereby significantly enriching our understanding of QCD and the nucleon structure. Recently, Ji, Ma and Yuan explicitly proved [7] that QCD factorization is valid for SIDIS with hadrons emitted in the current fragmentation region with low transverse momentum $p_{\perp h} \ll Q$. QCD factorization of spin-dependent cross sections in SIDIS and Drell-Yan has also been proved for the low $p_{\perp h}$ case [8].

The SMC experiment at CERN [2] extracted leading order quark spin-flavor information through SIDIS at $\langle Q^2 \rangle = 10$ GeV^2. The HERMES experiment at DESY recently published the results of a leading order spin-flavor decomposition at $\langle Q^2 \rangle = 2.5$ GeV^2, and for the first time extracted the sea quark polarizations [3]. Most recently, it was realized that target single-spin asymmetry in SIDIS can be used to access the Chiral-odd quark transversity distribution (h_{1q}). Moreover, information on quark spin-orbit correlation thus quark angular momentum can be accessed by extracting transverse momentum dependent distributions (TMDs), such as the Sivers functions ($f_{1q}^{\perp}$) in SIDIS. The recent HERMES [4] and COMPASS [5] measurements of SSA have generated a rapid new theoretical development in the study and understanding of the SIDIS process. In addition to model calculations of the transversity distributions and lattice calculations of the tensor charges, increasingly large efforts have been devoted to understanding the reaction mechanisms of the single-spin asymmetry from the fundamental theory of strong interaction, QCD. In particular, the rapid progress in the study of the Sivers effect and related mechanisms has brought our understanding to a new level. The link of the SIDIS SSA with other area of hadronic physics, such as in the Drell-Yan and $p\bar{p}$ reactions and multi-hadron production processes, has not only raised great interest in theoretical efforts, but also in experimental efforts. Studies of TMDs and transversity physics has become a major goal of a number of new facilities, including RHIC-spin, J-PARC in Japan,

PAX at the future Facility for Anti-proton and Ion Research (FAIR) at GSI, JLab 12 GeV, and the future electron-ion collider (EIC).

1.2 Opportunities of SIDIS experiments at JLab 12 GeV

The next US nuclear physics long range plan highlighted the study of quark transversity and transverse momentum dependent parton distributionsquark through SIDIS. Jefferson Lab 12 GeV upgrade will provide many of these unique opportunities, among them are:

- Transverse target single spin asymmetry measurements A_{UT} (on polarized proton, deuteron and ^{3}He) and extraction of Collins and Sivers moments to provide constrain on quark transversity, the T-odd Collins fragmentation functions and the Sivers distibutions for both $u-$ and d-quarks.

- Longitudianl beam-target double-spin asymmetry measurements A_{LL} (on polarized proton, deuteron and ^{3}He) to constrain quark hilicity distribution for each flavor separately and to access polarized sea asymmetry $\Delta\bar{u} - \Delta\bar{d}$.

- Measurements of hadron azimuthal distribution ($cos(2\phi)$) on unpolarized targets to access information on quark spin-orbit correlation by extracting the so-called Boer-Mulders functions.

- Measurements of other azimuthal moments in single spin asymmetry and double-spin asymmetry to extract TMDs to gain access on quark spin-orbit correlations, for example: $\cos(\phi_h - \phi_S)$ in A_{LT} and $\sin(2\phi_h)$ in A_{UL} etc.

- Measurements of unpolarized SIDIS cross sections to access unpolarized sea asymmetry $\bar{u} - \bar{d}$.

1.3 Interpretations of SIDIS data

The first step in realizing these ambitious SIDIS program at JLab 12 GeV is to firmly establish the evidences that at JLab kinematics SIDIS reactions can be interpretated in terms of parton distributions and fragmentation functions.

Within the statistical precisions of the HERMES and COMPASS experiments, SIDIS data have been interpretated in a self-consistent manner at the leading order, i.e.

$$\sigma^h(x, Q^2, z) = \sum_f q_f(x, Q^2) \cdot D_q^h(z, Q^2). \tag{1}$$

This naive x-z separation assumption has been shown to be working at $10 - 20\%$ level in understanding hadron multiplicities.

Recent JLab E00-108 data [6], on unpolarized SIDIS cross section ratios of proton and deuteron, also indicates that at the leading order naive x-z separation is not

far away from the reality. As shown in Fig. 1, ratios of combined SIDIS multiplicities of proton over deuteron are almost flat in the region of $0.3 < z < 0.7$. This apparent "precocious scaling" of quark-hadron duality suggests that at modest Q^2, information on the quark distributions is reasonably well-preserved in semi-inclusive reactions.

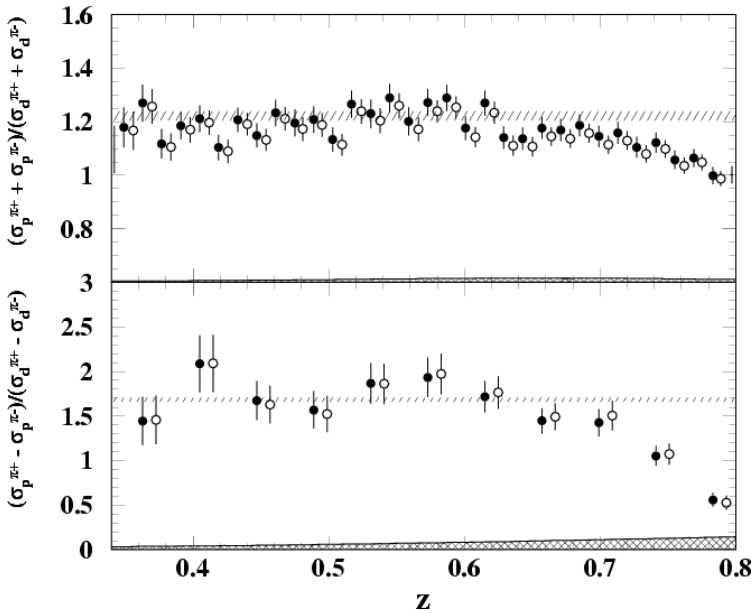

Figure 1: JLab Hall C SIDIS data at $E_0 = 5.5GeV$, $x = 0.32$ $Q^2 = 2.3$ GeV^2. Ratios of combined SIDIS multiplicities of proton over deuteron.

Since most of the TMD related terms in SIDIS contribute at a few percent level in cross sections, therefore, a detailed understanding of the cross sections, including their x, Q^2, z and P_t-dependencies, need to be clearly demonstrated to the next to leading order in QCD such that the extraction of new TMD physics not to be ruined by NLO QCD corrections.

At the next-to-leading order, following the well established formalism [11], tools of NLO global fits, which include data sets from e^+e^-, SIDIS and pp reactions, have become available recently [12]. Similar to other NLO PDF fits, these fits provide "uncertainties" in fragmentation functions such that SIDIS cross sections can be predicted with a theoritical "error band".

1.4 The goal of this experiment

The goal of this experiment is to provide precision data in SIDIS pion production and clearly establish the kinematic region of which JLab 12 GeV SIDIS data can be reliably interpreted, to the next leading order, in terms of parton densities and fragmentation functions.

This experiment will provide clear answers to the following questions: how well do we understand the fundemental cross sections in SIDIS and their relative relations

? and exactly how much the fraction of cross sections we don't understand beyond the next-to-leading order in QCD ?

2 Physics motivations

2.1 Spin-independent semi-inclusive DIS cross sections at NLO

The kinematics and the coordinate definition in SIDIS are illustrated in Fig. 2. We define E′ as the energy of the scattered electron and θ_e is the scattering angle, $\nu = E - E'$ is the energy transfer. The Bjorken-x, which indicates the fractional momentum carried by the struck quark, is defined as: $x = Q^2/(2\nu M_N)$, M_N is the nucleon mass. The momentum of the outgoing hadron is p_h and the fraction of the virtual photon energy carried by the hadron is: $z = E_h/\nu$. The hadron transverse momentum relative to $\vec{q}$ is labeled as $P_{h\perp}$ as shown in Fig. 2.

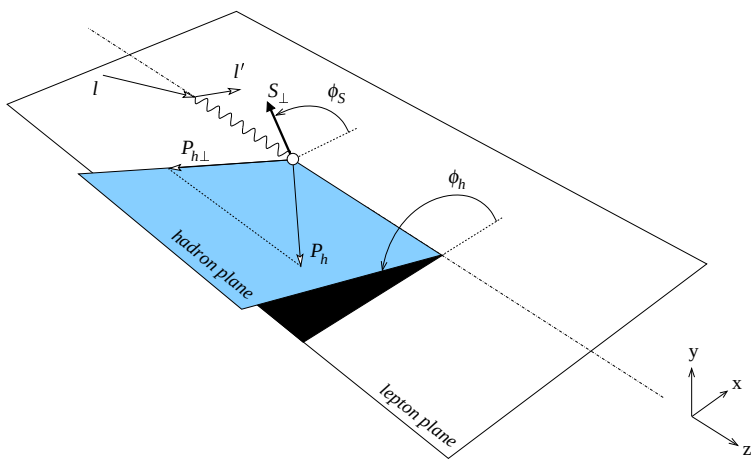

Figure 2: The definition of SIDIS kinematics, according to the Trento conventions.

The naive $x - z$ separation is not valid at the next-to-leading order when the one-gluon diagrams in Fig. 3 are considered. However, the exact form of these terms has been well-known [13]. At NLO, the terms of $q(x) \cdot D(z)$ in Eq. 1 are added with the double convolutions of the type $q \otimes \mathcal{C} \otimes D$ in which $\mathcal{C}$ are well-known Wilson coefficients [14]:

$$[q \otimes C \otimes D](x, z) = \int_x^1 \frac{dx'}{x'} \int_z^1 \frac{dz'}{z'} q\left(\frac{x}{x'}\right) C(x', z') D\left(\frac{z}{z'}\right). \tag{2}$$

Not only are x and z mixed through the double convolutions at the next-to-leading order, the unpolarized cross section σ^h also depends on the virtual photon variable $y = (E_0 - E')/E_0$ due to the longitudinal component of the virtual photon.

We define the short-hand notation:

$$qD + \frac{\alpha_s}{2\pi} q \otimes C \otimes D = q\left[1 + \otimes \frac{\alpha_s}{2\pi} C \otimes\right] D, \tag{3}$$

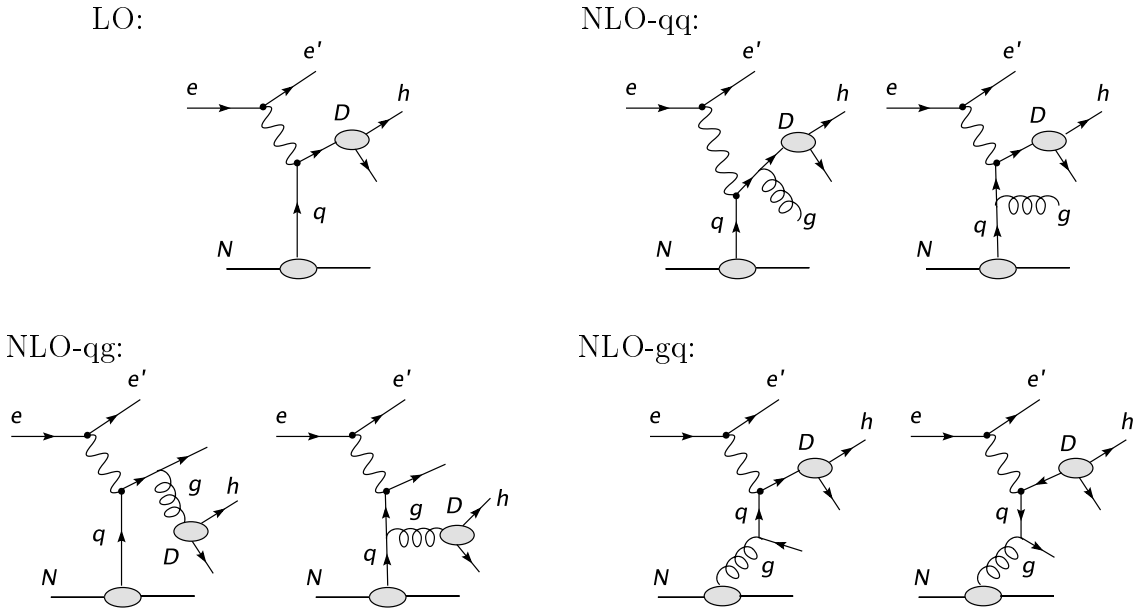

Figure 3: Semi-inclusive deep inelastic scattering diagrams at leading order (LO) and the next-to-leading order (NLO).

at NLO instead of Eq. 1, we have:

$$\sigma^h(x,z) = \sum_f e_f^2 q_f \left[1 + \otimes \frac{\alpha_s}{2\pi} \mathcal{C}_{qq} \otimes\right] D_{q_f}^h + \left(\sum_f e_f^2 q_f\right) \otimes \frac{\alpha_s}{2\pi} \mathcal{C}_{qg} \otimes D_G^h + G \otimes \frac{\alpha_s}{2\pi} \mathcal{C}_{gq} \otimes \left(\sum_f e_f^2 D_{q_f}^h\right), \quad (4)$$

where $q_f(x)$ is quark distribution function of flavor f. The functions $D_{q_f}^h(z)$ represent the probability that a quark f fragments into a hadron h. For any given set of PDFs, SIDIS cross sections can be calculated numerically [11] according to Eq. 4. It is also well-known that in Mellin-n space, the double-convolutions factorize into simple products under moments, and the parton distributions can be recovered by an inverse Mellin transformation and all moments of Wilson coefficients are already calculated [15].

2.2 NLO global fit of fragmentation functions.

Our knowledge of parton fragmentation functions has traditionally come from fits of existing e^+e^- data. In a recent work [?], the frist attempt was made to including data sets of e^+e^- as well as SIDIS and pp reactions in a NLO global fit. As shown in Fig. fig:nlofit1, the new fit reproduced HERMES SIDIS charged pion multiplicity data reasonablly well.

Following the NLO global fit [?], SIDIS cross sections at JLab 12 GeV kinematics are predicted for this experiment, with theory "error band". When new high precision

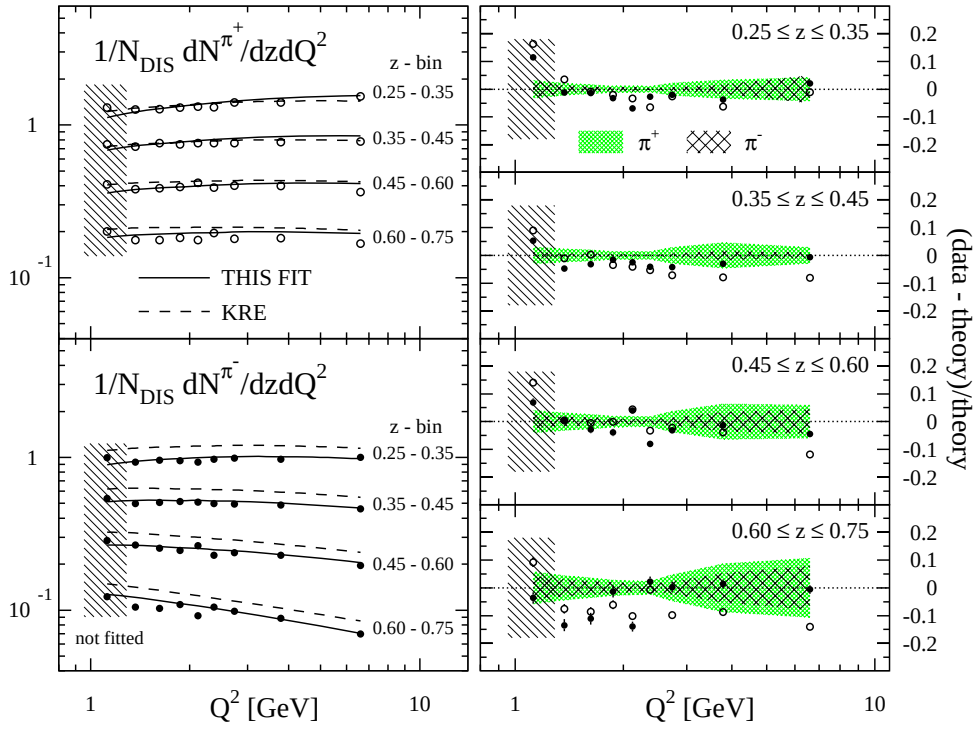

Figure 4: HERMES charged pion multiplicity data compared with NLO global fit.

data become available from this experiment, new constraints on the global fit will significantly reduce the present "error band", and detailed $p_\perp^h$ and azimuthal angle dependence can be studied to extract new physics.

2.3 Experimental observables of this experiment

In this experiment, the following observables will be measured:

Pion multiplicities

The multiplicity of hadron h produced at a fixed momentum fraction z in SIDIS reaction is defined as:

$$\frac{\sigma^h(x,z,Q^2)}{\sigma_{DIS}} = \frac{1}{\sigma_{DIS}} \int \frac{d\sigma^h}{d\Omega_h d^2P_t^h}\, d\Omega_h\ d^2P_t^h \tag{5}$$

It is a ratio of SIDIS cross section over the inclusive DIS cross section and covers all hadron angle and transverse momentum. Notice that in practice, the scattered electron's solid angle and detection efficiency do not enter into the measurements of hadron multiplicity.

Ratios of charged pion multiplicities

We define observable r as ratio of π^- and π^+ multiplicities:

$$r(x,z,Q^2) = \frac{\sigma^{\pi^-}}{\sigma^{\pi^+}} \tag{6}$$

Combined charged pion multiplicities

The combined charged pion multiplicity is defined as:

$$\frac{\sigma^{\pi^+ + \pi^-}}{\sigma_{DIS}}(x,z,Q^2) = \frac{1}{\sigma_{DIS}}\left(\sigma^{\pi^+} + \sigma^{\pi^-}\right). \tag{7}$$

Ratios of proton over deuteron combined charged pion multiplicities

We define observable r^+ and r^- as ratio of combined multiplicities between proton and deuteron targets:

$$r^+(x,z,Q^2) = \frac{\sigma_p^{\pi^+} + \sigma_p^{\pi^-}}{\sigma_d^{\pi^+} + \sigma_d^{\pi^-}} \tag{8}$$

$$r^-(x,z,Q^2) = \frac{\sigma_p^{\pi^+} - \sigma_p^{\pi^-}}{\sigma_d^{\pi^+} - \sigma_d^{\pi^-}}. \tag{9}$$

SIDIS cross sections

When care is taken in determine the absolute luminosity, the scattered electron's solid angles and detection efficiencies, absolute cross sections of SIDIS hadron production can be extracted from this experiment. Although the goal of this experiment is to measure ratios of cross sections, extensive calibration runs will be taken such that the absolute cross sections can be determined as by-products.

3 This Experiment

The technical details of this experiment.

3.1 The CLAS12 detector

Nominal luminosity.

3.2 Electron detection

PID, efficiency.

3.3 Hadron detection

PID. π/K and π^+/p separation. π^0 detection. Resolution.
calibration of charged pion detection efficiency.

3.4 Hadron phase space differences

3.5 Vertex reconstruction

3.6 Targets density and luminosity corrections

3.7 Trigger and background

3.8 Kinematic coverage of SIDIS reaction with the CLAS12 detector

The definitions of the kinematic variables are the following: Bjorken-x, which indicates the fractional momentum carried by the struck quark, is $x = Q^2/(2\nu M_N)$, where M_N is the nucleon mass. The momentum of the outgoing pion is p_π and the fraction of the virtual photon energy carried by the pion is: $z_\pi = E_\pi/\nu$. W is the invariant mass of the whole hadronic system and W' is the invariant mass of the hadronic system without the detected pion. We have:

$$\begin{aligned} W^2 &= M_N^2 + Q^2(\frac{1}{x} - 1), \\ W'^2 &= (M_N + \nu - E_\pi)^2 - |\vec{q} - \vec{p}_\pi|^2. \end{aligned} \tag{10}$$

SIDIS cuts.
Phase space.

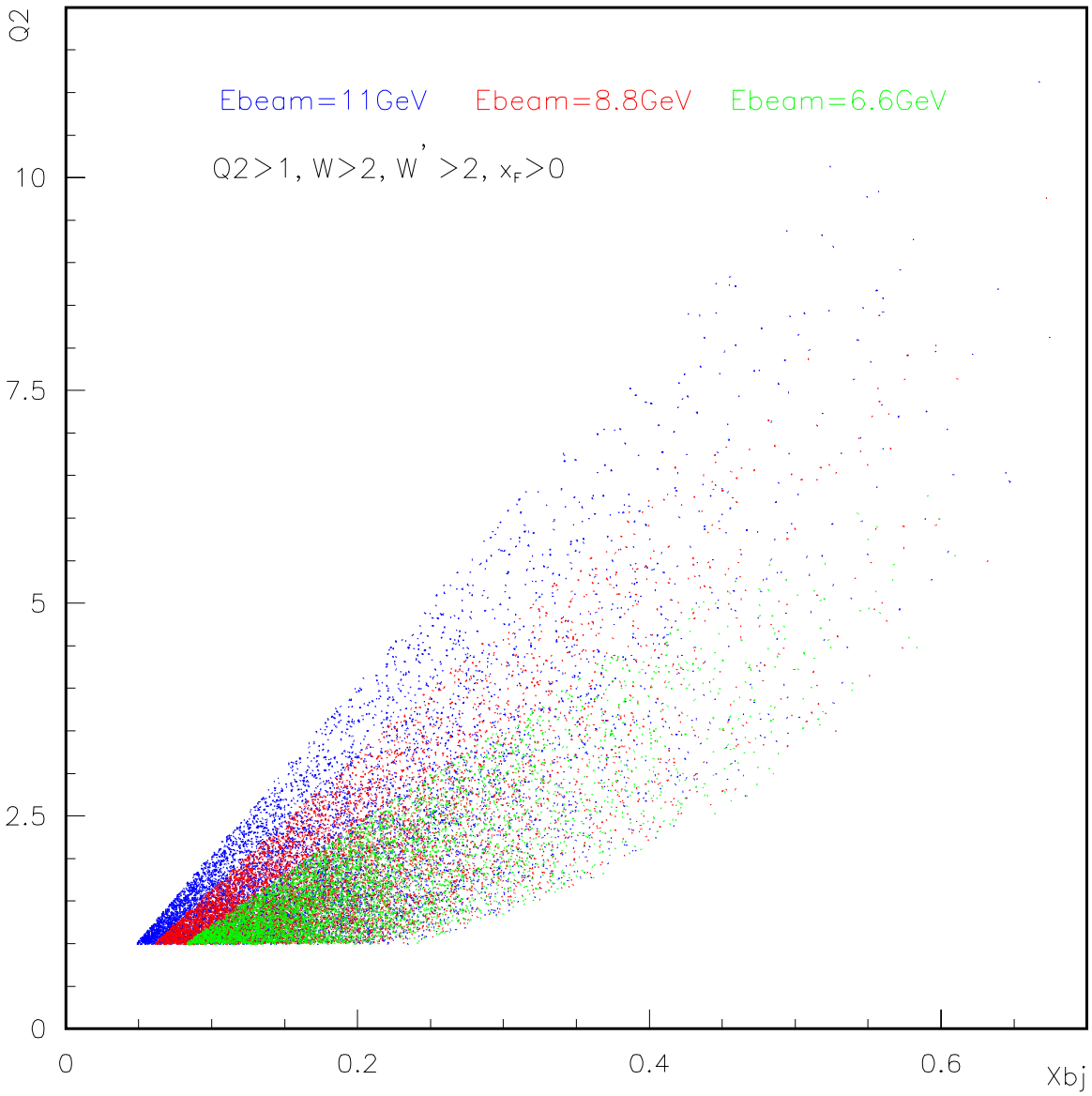

Figure 5: SIDIS phase space coverage of (Q^2,x_{bj}) for E_0=11, 8.8 and 6.6 GeV. The total number of events is not to scale.

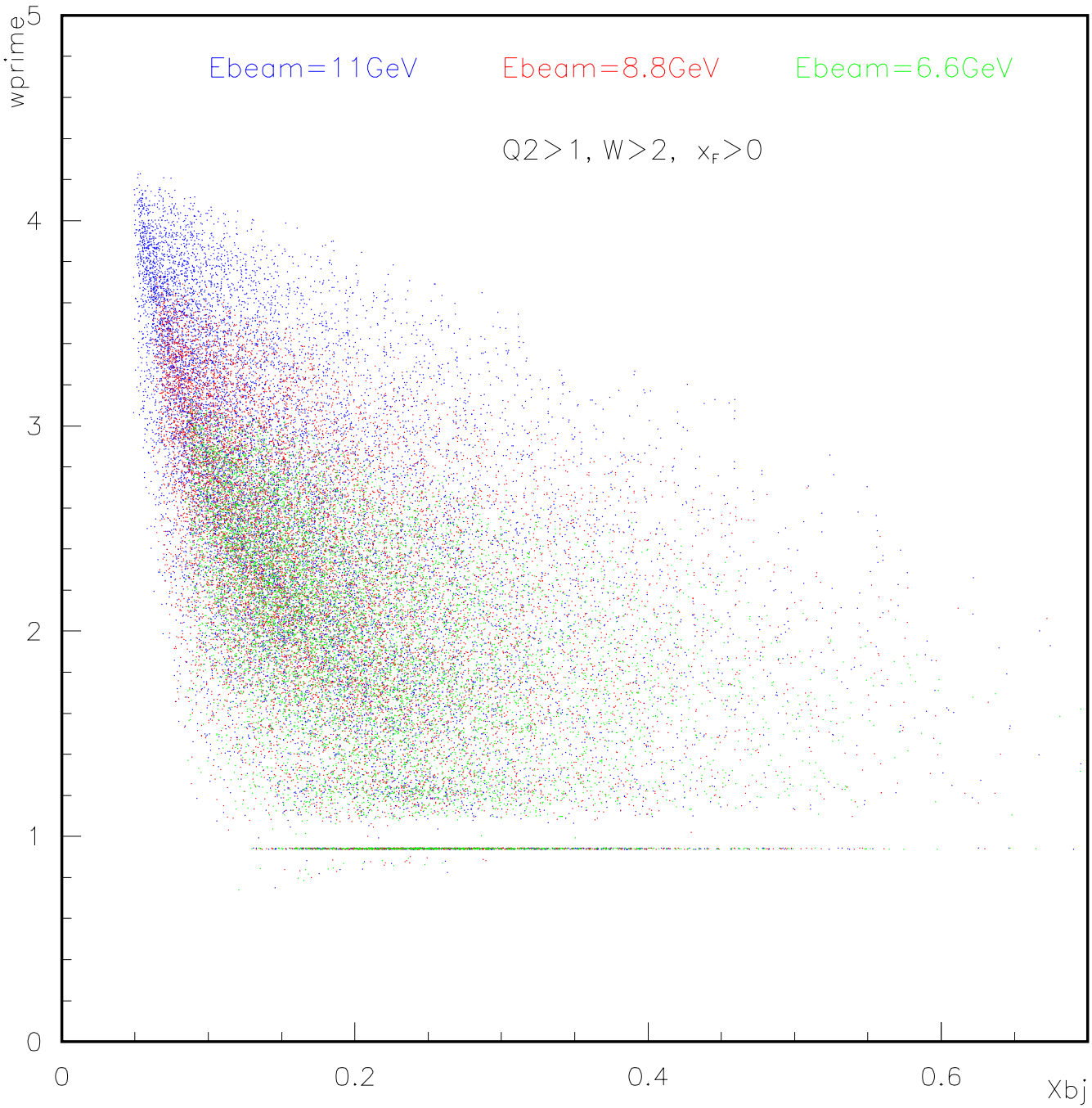

Figure 6: SIDIS phase space coverage of (W',x_{bj}) for E_0=11, 8.8 and 6.6 GeV.The total number of events is not to scale.

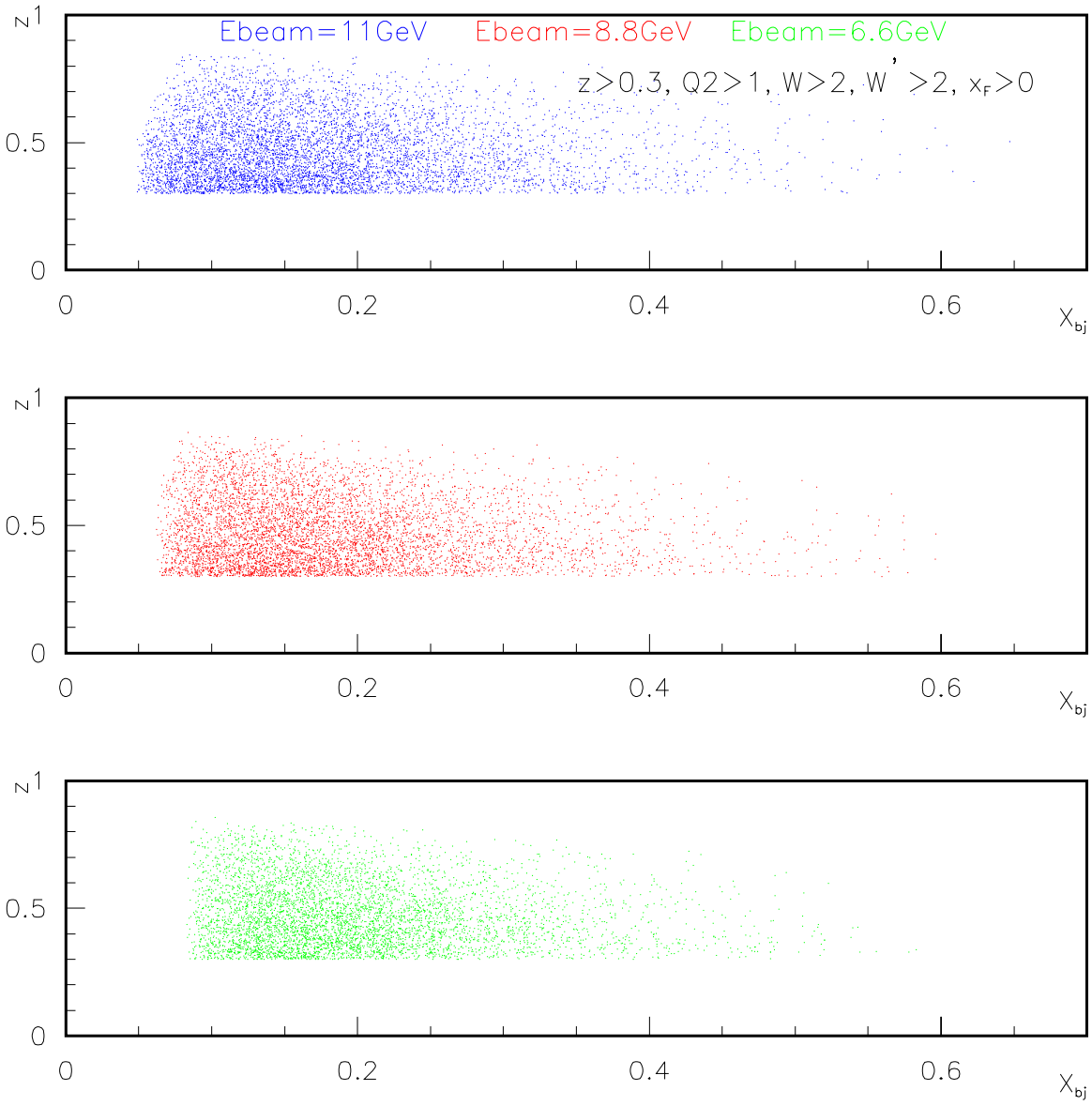

Figure 7: SIDIS phase space coverage of (z_π,x_{bj}) for E_0=11, 8.8 and 6.6 GeV.The total number of events is not to scale.

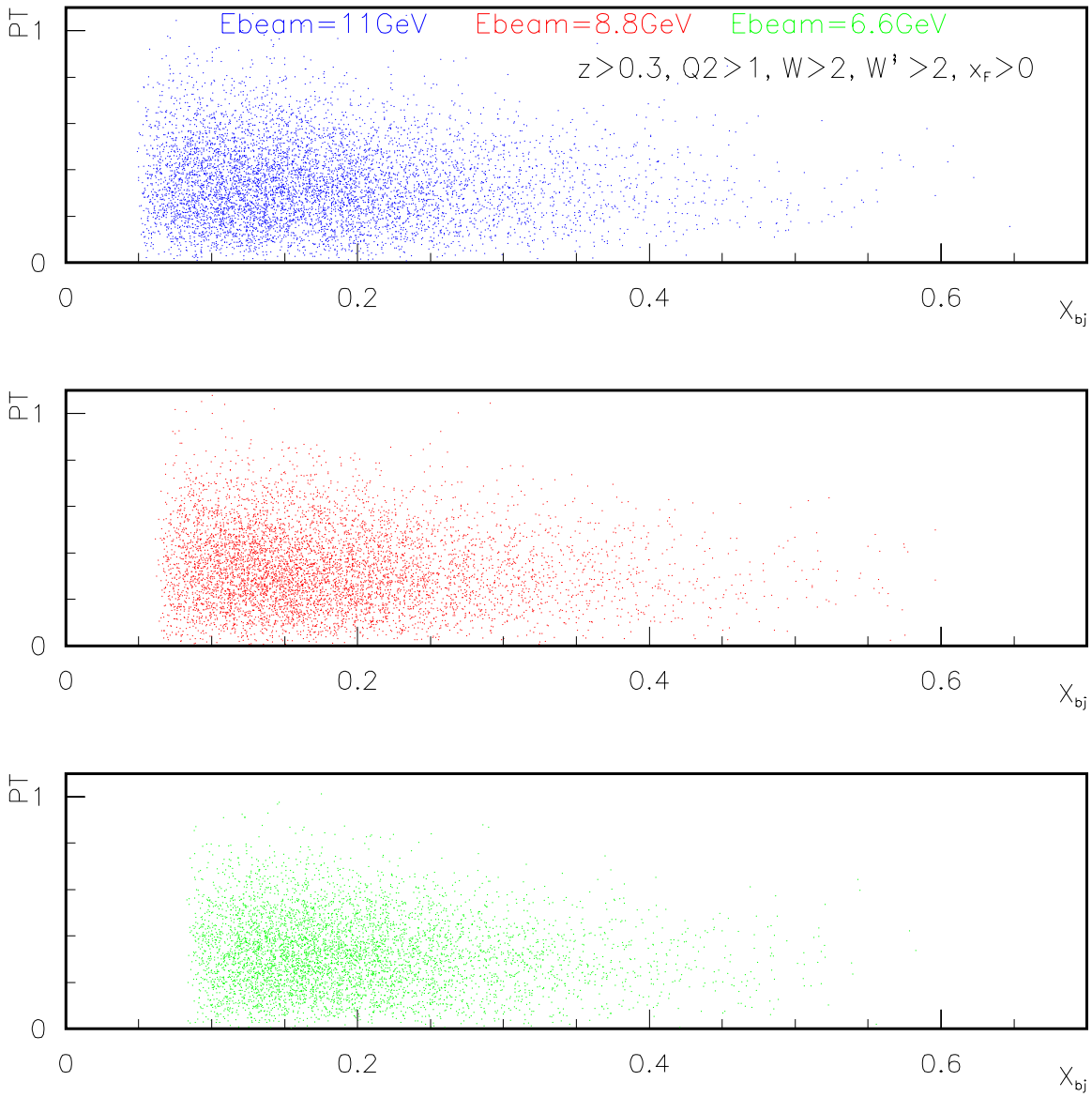

Figure 8: SIDIS phase space coverage of (p_t^π,x_{bj}) for E_0=11, 8.8 and 6.6 GeV.The total number of events is not to scale.

4 Event Rate Estimate and Projected Uncertainties

4.1 Cross section and rate estimate

The estimation of the coincidence cross sections has the following inputs:

- The inclusive $p(e, e')$ cross sections.
- Parametrization of the fragmentation functions D_π^+ and D_π^-.
- A model of the transverse momentum distributions of pion and kaon as fragmentation products.

The inclusive deep inelastic (e, e') cross section can be expressed in the quark parton model as:

$$\frac{d^2\sigma}{d\Omega dE'} = \frac{\alpha^2(1+(1-y)^2)}{sxy^2}\frac{E'}{M_N\,\nu}\sum_{q,\bar{q}} e_q^2 f_1^q(x), \tag{11}$$

where $s = 2E\,M_N + M_N^2$. The unpolarized quark distribution functions $f_1^q(x)$ and $f_1^{\bar{q}}(x)$ are taken from the CTEQ global fits [?]. The semi-inclusive $(e, e'h)$ cross section relates to the quark fragmentation function $\mathrm{D}_q^h(z)$ and the total inclusive cross section σ_{tot} through:

$$\frac{1}{\sigma_{tot}}\frac{d\sigma(e,e'h)}{dz} = \frac{\sum_{q,\bar{q}} e_q^2 f_1^q(x) D_q^h(z)}{\sum_{q,\bar{q}} e_q^2 f_1^q(x)}. \tag{12}$$

Existing data indicate that the fragmented products follow a Gaussian-like distribution in transverse momentum.

Monte Carlo simulation to estimate the count rates.

Luminosity 10^{35} cm^{-2}s^{-1}. Compare with HERMES event rate.

The issue of hadron decay is considered in the Monte Carlo.

Check the normalization point.

4.2 Statistics compared with HERMES data

4.3 Systematic uncertainties

All ratios.

Absolute cross section assume systematical uncertainties of $\pm 5\%$.

Relative systematic uncertainties

5 Luminosity and beam time assumptions

Following the technical details outlined in the CLAS12 technical design report, we have assumed a nominal luminosity of 10^{35} cm^{-2}s^{-1} in our event rate estimation.

The beam time needed for this experiment are listed in Table 1. The physics production with a 11 GeV beam for 1000 hours each on unpolarized liquid hydrogen and deuterium targets are assumed. These nominal 11 GeV production beam time will be shared between several physics programs including DVCS, deeply-virtual meson production, beam SSA in SIDIS, azimuthal asymmetries in SIDIS. These beam time allocations will not be driven by this proposal.

In addition, nominal 250 hours each on hydrogen and deuterium targets for 8.8 and 6.6 beam are assumed for estimation of statistics. Again, these beam time allocations will be driven by the needs of other low rate physics program.

	E_0=11 GeV	E_0=8.8 GeV	E_0=6.6 GeV
Beam on LH_2	1000 hours	250 hours	250 hours
Beam on LD_2	1000 hours	250 hours	250 hours

Table 1: Nominal beam time assumption.

6 Expected Results

6.1 SIDIS pion multiplicities, z-dependence

6.2 Q^2 dependence of pion multiplicities

6.3 Ratios of combined charged-pion multiplicities

6.4 $P_\perp$ dependence of pion production

$P_\perp$ dependence of the fragmentation functions

6.5 Singlet and non-singlet fragmentation functions

6.6 Valence quark distribution ratio d_v/u_v

7 By-products

7.1 SIDIS charged kaon multiplicities, z-dependence

7.2 $\cos\phi$ and $\cos 2\phi$ moments

7.3 Multiplicities of ρ, K_s^0 and ϕ mesons

7.4 Multiplicities of p, $\bar{p}$, Λ and other hyprons

7.5 Beam single-spin asymmetry A_{LU}

7.6 Absolute cross sections

8 Relation with other experiments

- HERMES experiment

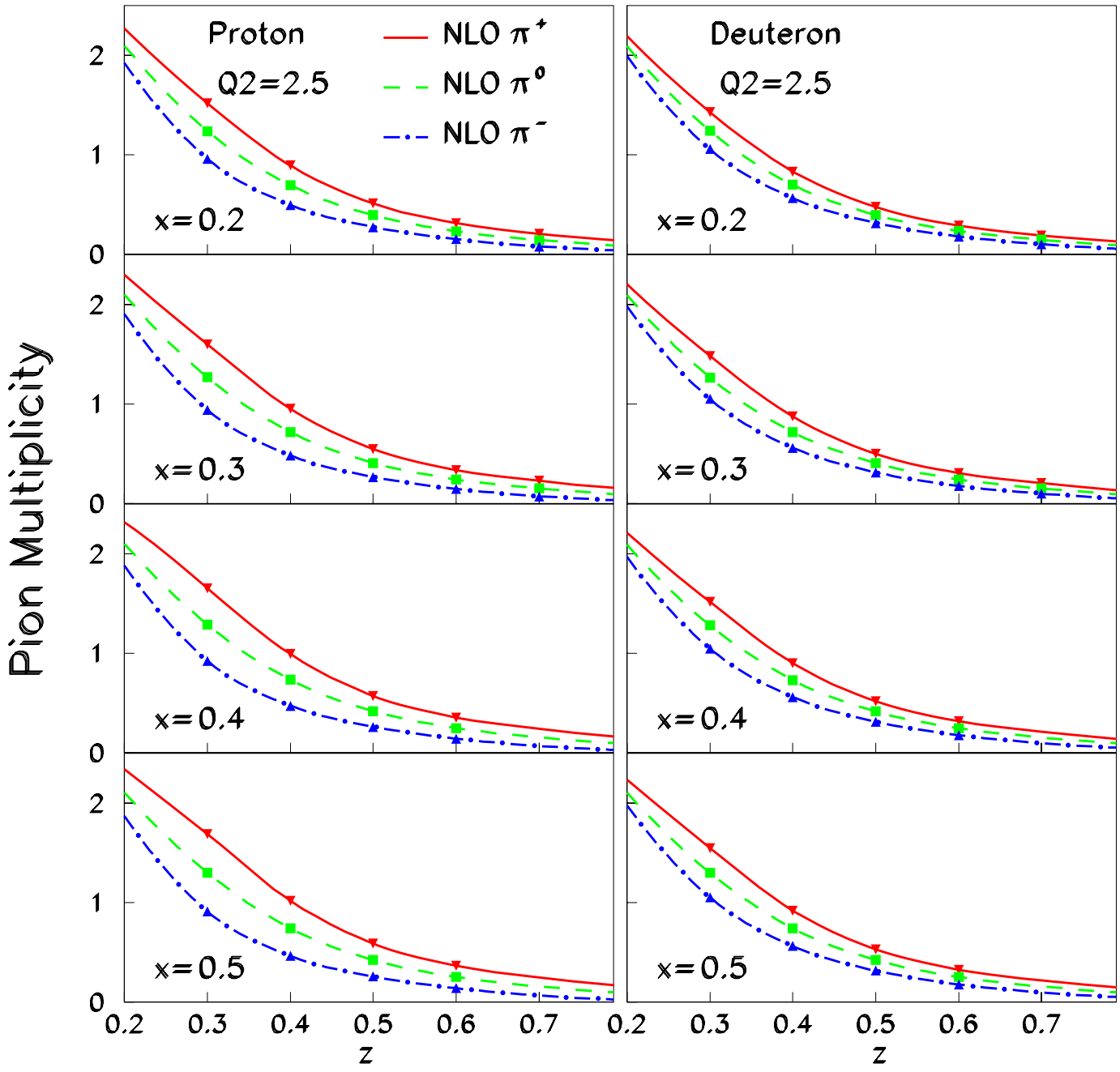

Figure 9: One example of z-dependence of pion multiplicities for bin $Q^2 = 2.5$ GeV^2, E$_0$=11 GeV.

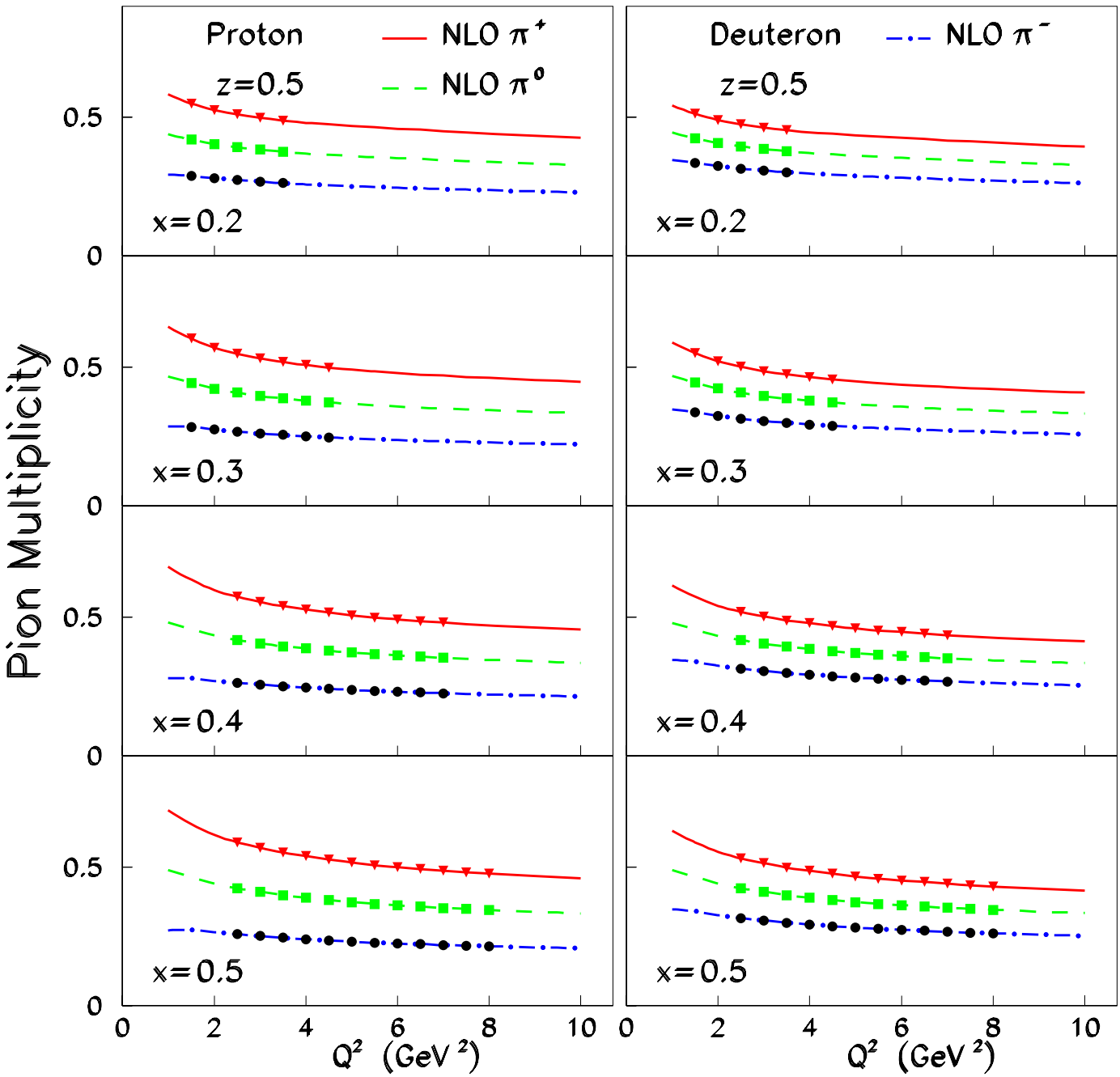

Figure 10: One example of Q^2 dependence of pion multiplicities for bin $z = 0.5$, E_0=11 GeV.

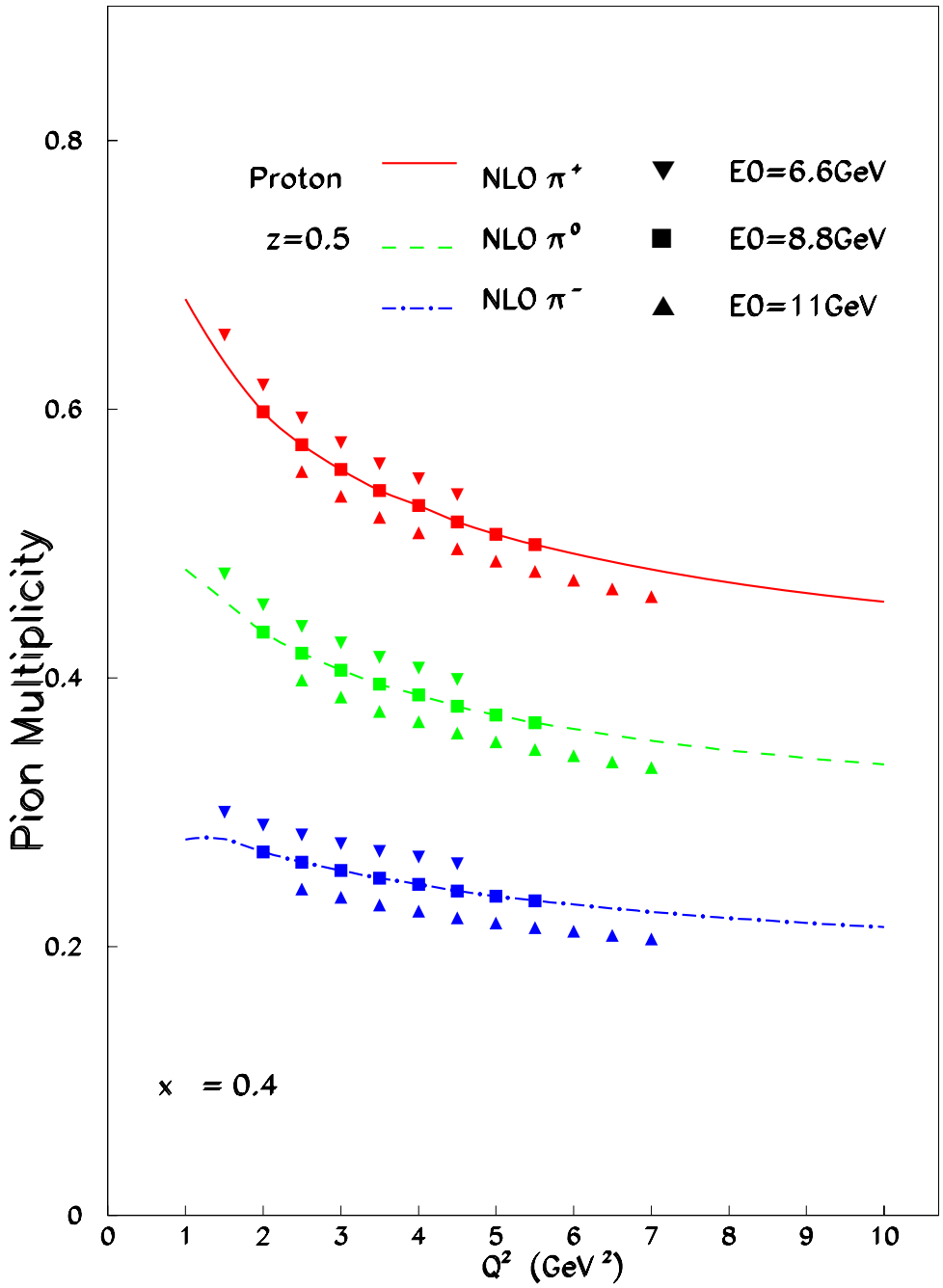

Figure 11: A zoomed-in view of Q^2 dependence of pion multiplicities for bin $z = 0.5$ and $x = 0.4$, E_0=11, 8.8 and 6.6 GeV.

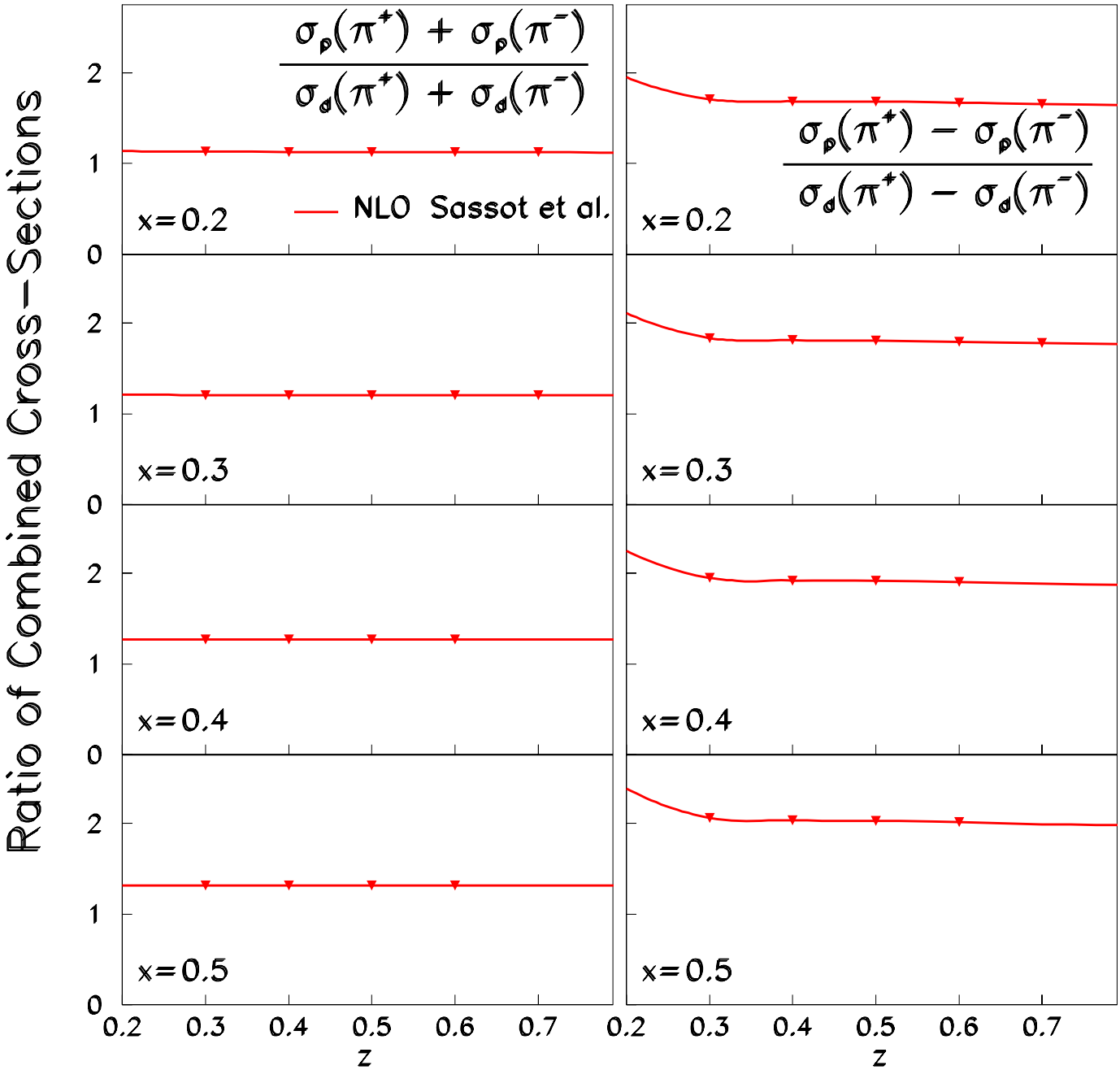

Figure 12: One example of z-dependence of ratio of combined charged-pion multiplicities for bin $Q^2 = 2.5$ GeV^2, E$_0$=11 GeV.

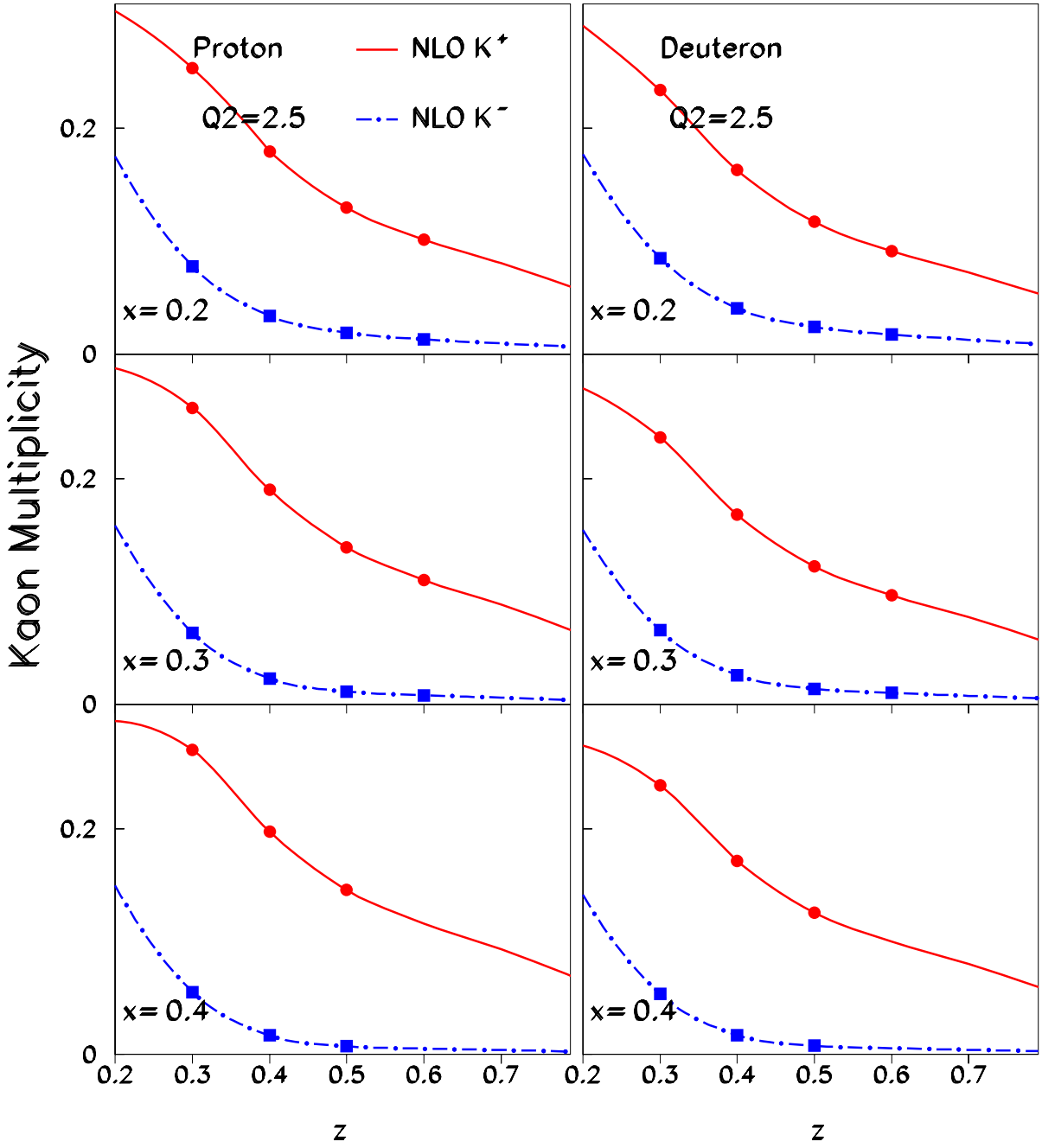

Figure 13: One example of z-dependence of kaon multiplicities for bin $Q^2 = 2.5$ GeV^2, E$_0$=11 GeV.

- COMPASS experiment
- BELLE experiment
- JLab-12 GeV at Hall C. Measurement of R
- JLab 12 GeV at Hall A. Polarized ^{3}He measurements.
- Other CLAS12 proposals. Polarized and unpolarized targets.

9 Summary

This experiment will provide clear answers to the following questions: how well do we understand the fundemental cross sections in SIDIS and exactly how much the fraction of cross sections we don't understand beyond the next-to-leading order in QCD ?

10 Acknowledgment

We thank D. de Florian, R. Sassot and M. Stratmann for providing their NLO calculations.

A Details of Monte Carlo simulations

The phase space coverage is obtained from a detailed Monte Carlo simulation which includes realistic For the purpose of estimating kinematic distributions and event rates, the LEPTO program was used. The simulation was performed in two steps. First, for each setting and target different reaction products were generated. Second, the events were read back by an analyzer which produced histograms for each hadron species within the constraints of the angular and momentum acceptances of CLAS12GeV.

The cuts SIDIS events are set at $Q^2 > 1(GeV/c)^2$ and $W > 2GeV$ to meet the requirement of x-scaling. $x_F > 0$ is used to select those hadrons from current fragmentation. The momentum for hadrons are required to be higher than $1GeV$ and the invariant mass of the undetected system is required as $W' > 1.5GeV$

Fig. 14 to Fig. 17 show some observables distributions generated from the LEPTO code for π with the SIDIS cuts. Some observables for kaon are shown in Fig. **??**.

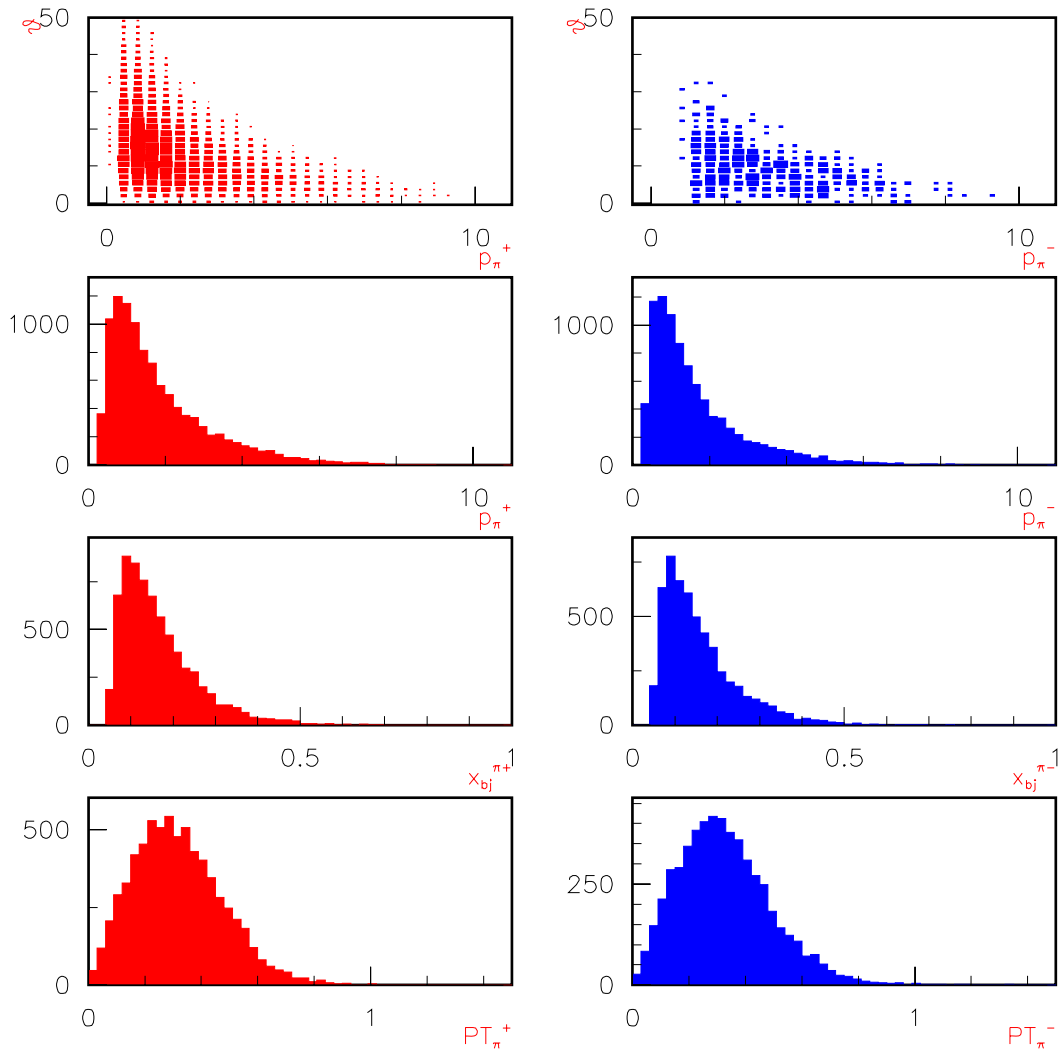

Figure 14: Hadron spectra (polar angle vs. momentum, momentum, x, and PT) for π^+(left) and π^-(right) from the LEPTO code assuming $\theta_e = 20°$, ν =7 GeV, a 1 GeV electron beam, and a deuteron target.

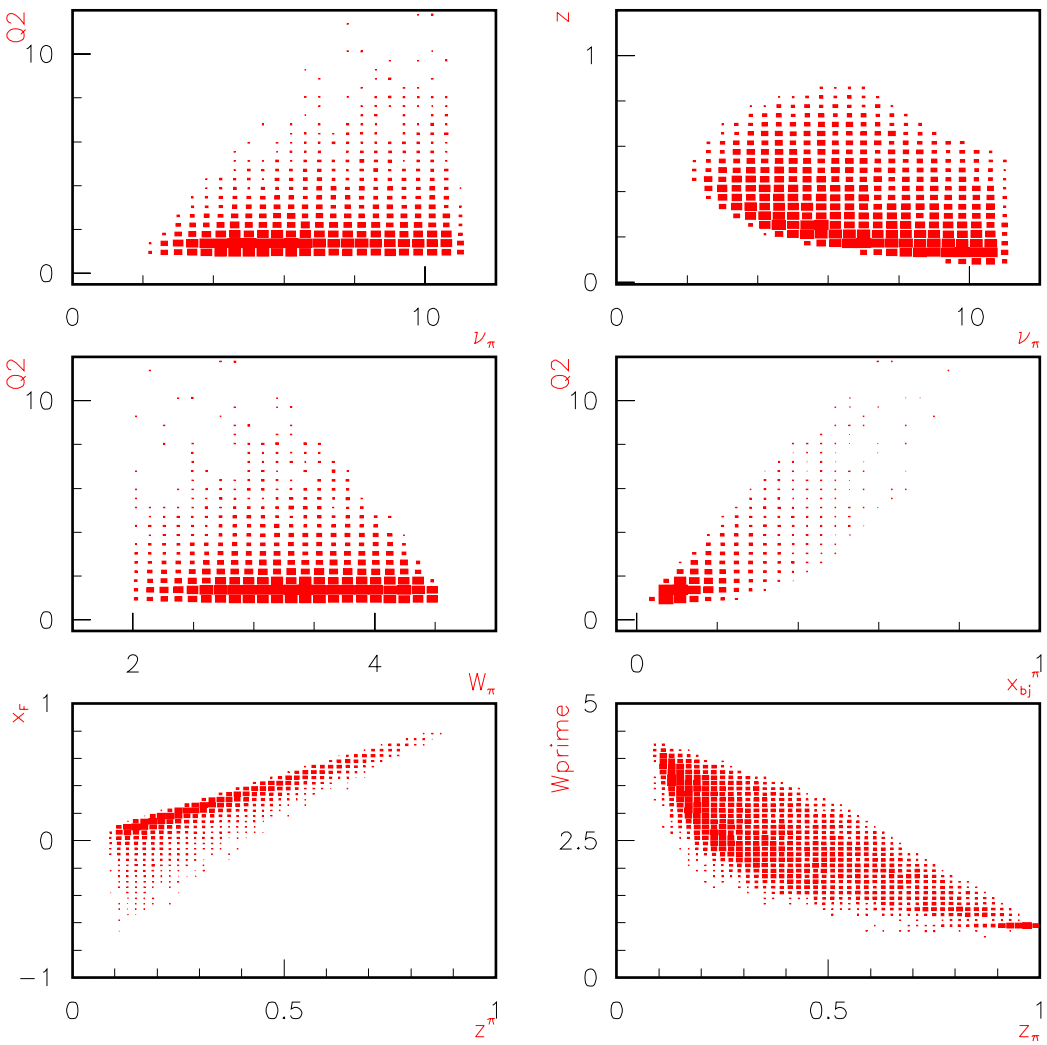

Figure 15: Hadron spectra (Q^2 and z vs. ν, Q^2 vs. W and x_{bj}, x and W' vs. z) for π from the LEPTO code assuming $\theta_e = 20°$, ν =7 GeV, a 1 GeV electron beam, and a deuteron target.

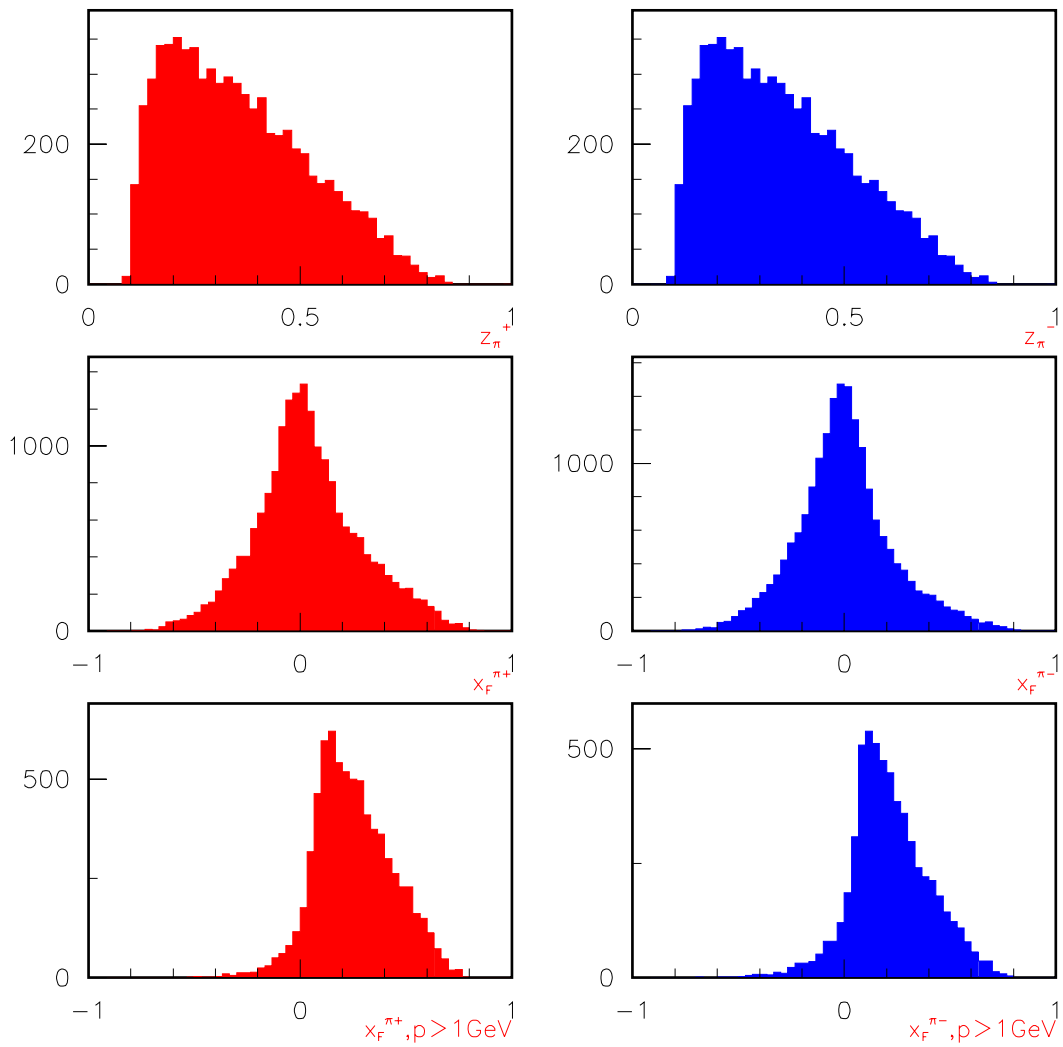

Figure 16: Hadron spectra (z, x_F, and x_F while p_π >1GeV) for π^+(left) and π^-(right) from the LEPTO code assuming $\theta_e = 20°$, ν =7 GeV, a 1 GeV electron beam, and a deuteron target.

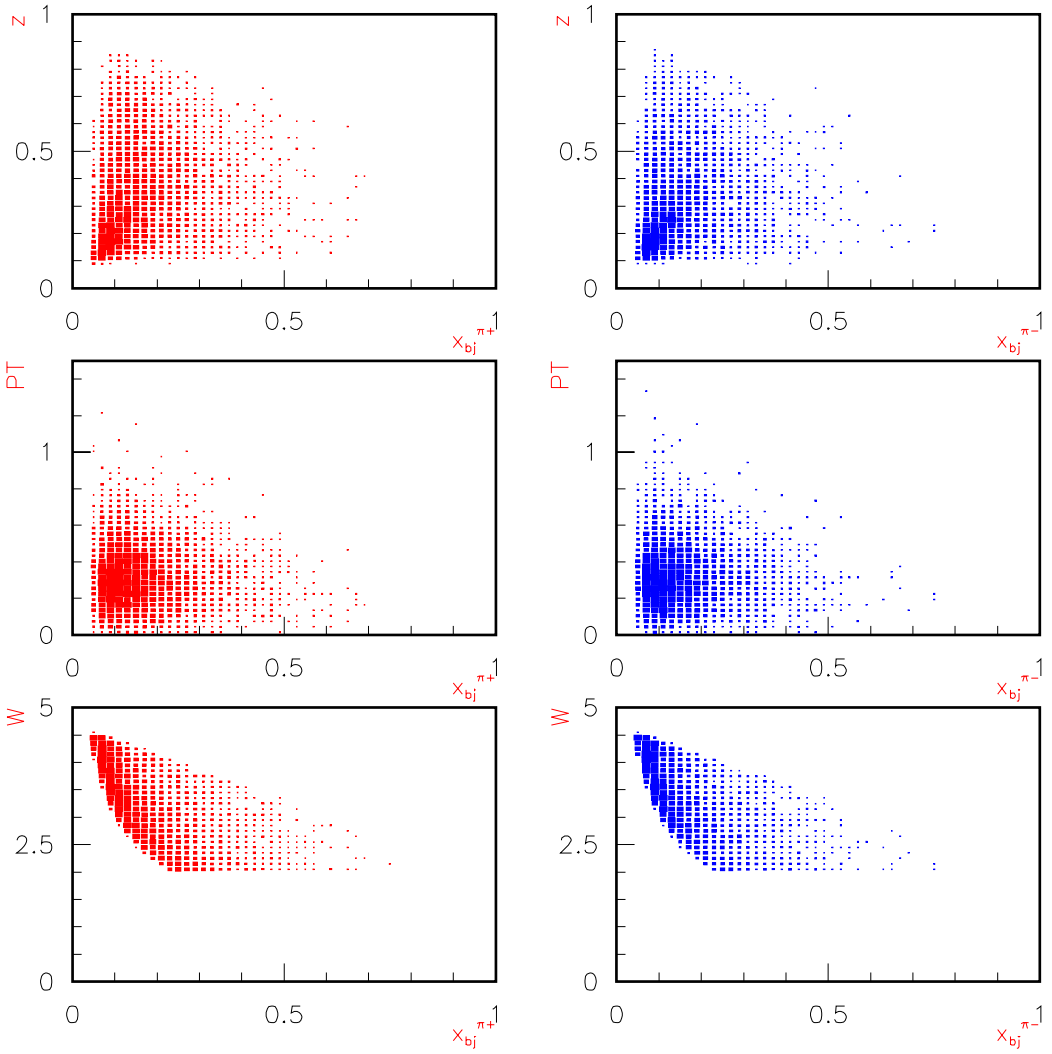

Figure 17: Hadron spectra (z, PT and W vs. x_{bj}) for π from the LEPTO code assuming $\theta_e = 20°$, ν =7 GeV, a 1 GeV electron beam, and a deuteron target.

References

1. L. L. Frankfurt, M. I. Strikman, L. Mankiewicz, A. Schafer, E. Rondio, A. Sandacz and V. Papavassiliou, Phys. Lett. B **230**, 141 (1989); F. E. Close and R. G. Milner, Phys. Rev. D **44**, 3691 (1991).
2. The Spin Muon Collaboration, *Phys. Lett.* B **420**, 180 (1998).
3. HERMES collaboration, *Phys. Rev. Lett.* **92**, 012005 (2004), and *Phys. Rev.* D **71**, 012003 (2005).
4. A. Airapetian *et al.*, Phys. Rev. Lett. **94**, 012002 (2005).
5. V. Y. Alexakhin *et al.*, Phys. Rev. Lett. **94**, 202002 (2005).
6. R. Ent. Phys. Rev. Lett.
7. Xiangdong Ji, Jian-Ping Ma and Feng Yuan, hep-ph/0404183.
8. Xiangdong Ji, Jian-Ping Ma and Feng Yuan, hep-ph/0405085.
9. P. Mulders and R. D. Tangerman *Nucl. Phys.* B **461**, 197 (1996)
10. X. D. Ji, J. P. Ma and F. Yuan, Phys. Rev. D **71**, 034005 (2005). Phys. Lett. B **597**, 299 (2004).
11. D. de Florian and R. Sassot, *Phys. Rev.* D **62**, 094025 (2000), and D. de Florian, O. A. Sampayo and R. Sassot, *Phys. Rev.* D **57**, 5803 (1998)
12. D. de Florian, G. A. Navarro and R. Sassot, *Phys. Rev.* D **71**, 094018 (2005), and private communications (2005).
13. D. Graudenz, *Nucl. Phys.* B **432**, 351 (1994).
14. D. de Florian, C. A. Garcia Canal, R. Sassot, *Nucl. Phys.* B **470**, 195 (1996).
15. Marco Stratmann and Werner Vogelsang, *Phys. Rev.* D **64**, 114007 (2001)
16. J. C. Collins and A. Metz, Phys. Rev. Lett. **93**, 252001 (2004).
17. D. Boer and P. Mulders, *Phys. Rev.* D **57**, 5780 (1998)
18. F. Yuan, Phys. Lett. **B575**, 45 (2003), and private communications (2006).
19. J. C. Collins, Phys. Lett. B **536** (2002) 43.
20. R. Kundu and A. Metz, Phys. Rev. D **65** (2002) 014009.
21. Alessandro Bacchetta, Umberto D'Alesio, Markus Diehl, C. Andy Miller, *Phys. Rev.* D **70**, 117504 (2004).
22. A. Bacchetta, hep-ph/0307282.
23. S. Wandzura and F. Wilczek, Phys. Lett. **B72**, 195 (1977).
24. S. Kretzer, Phys. Rev. D **62**, 054001 (2000).
25. B. A. Kniehl, G. Kramer, and B. Potter, *Nucl. Phys.* B **582**, 514 (2000).